GE Casting Project

M. F. X. Gigliotti (gigliotti@crd.ge.com, 518-387-6356)
S.-C. Huang (huangsc@crd.ge.com, 518-387-5380)
F. J. Klug (klug@crd.ge.com 518-387-7304)
A. M. Ritter (ritter@crd.ge.com 518-387-7621)
General Electric Corporate Research and Development
One Research Circle
Niskayuna, NY 12309-1027

Abstract

Directionally solidified and single-crystal airfoils—with complex internal cooling designs—are being introduced into large land-based gas turbine engine applications. The requirements for grain perfection and those for accurate part geometry compete with one another and create formidable challenges to successful, widespread use of large directionally solidified and single-crystal parts.

The overall technical objective of this project is to achieve a cost-effective yield of single-crystal and directionally solidified components by: evaluating and implementing liquid-metal cooling (LMC) directionally solidified processing, which will provide a higher yield process; and adapting new alumina core formulations, which will provide cores with physical and mechanical properties that reduce casting related defects.

Liquid metal cooling will provide increased thermal gradients without increasing casting metal temperature by improving heat input and removal from castings. A GE-PCC Airfoils, Inc. team, using a pilot LMC furnace - designed in collaboration with ALD Vacuum Technologies and installed at GE, is conducting this work. Development of cores with improved capabilities will be achieved by combining industrial core fabrication technology with unique alumina core chemistries. This will provide a core capable of being used at higher casting temperatures. GE will validate the alumina ceramic formulations with commercial raw materials and apply industrial shape-making techniques to this alumina composition. Major core manufacturers will then adapt this development within their own facilities.

For LMC directional solidification processing, results of casting trials made in the LMC furnace, a preliminary process window, an assessment of process viability, and the experimental plans for identification of the optimal process window and conducting an economic analysis will be reported. For alumina cores, the results of statistically designed experiments to optimize core microstructure and properties will be reported. Core microstructures and properties, as a function of compositional and process variables will be presented. This work is carried out under subcontract 85XSZ581C, period of performance 18 March 1998 through 30 September 2000, and Lockheed Martin project manager B. Radhakrishnan.

1. Development of an Alumina core for Investment Casting of Gas Turbine Hardware

1.1 Core Requirements and Process Selected

Stringent dimensional tolerances on gas turbine nozzles and blades have led to the need for improved dimensional control of the ceramics used in the casting process. Alumina cores have been developed as replacement for the traditional silica cores because:

1. Alumina is phase stable; in comparison, vitreous silica converts to cristobalite and has a destructive martensitic phase change on cooling.
2. Alumina can be fully sintered so that additional shrinkage does not occur during the casting process. Silica can only be partially sintered before casting and has significant shrinkage during the casting process.
3. The thermal expansion of alumina is similar the thermal expansion of the shell mold; silica's thermal expansion is a poor match for the thermal expansion of the shell mold.
4. Alumina has greater chemical stability than silica to reactive alloys containing Y and Hf.
5. Alumina has a higher melting point than silica which translates into the potential of use at higher casting temperatures.

A comparison of some of the properties of alumina and silica is shown in Table I. The superior properties of alumina are expected to result in economically significant improvements in casting yield and product quality. The program goals for the core research are to achieve acceptable high temperature mechanical properties with superior geometrical precision while satisfying the required surface finish and core removal requirements.

Table I

Core Materials

Material	Melting point	ΔG $kJ \cdot mol^{-1}\ O_2$ $1227°C\ (2240°F)$	$\alpha,\ \cdot 10^{-6}$ RT to 1300°C $(2370°F)$
SiO_2	1710°C 3110°F	640	~0.5/°C[†] ~0.9/°F[†] [†]vitreous
Al_2O_3	2050°C 3722°F	770	9/°C 16/°F

Gel casting, a manufacturing process pioneered at Oak Ridge National Laboratory (ORNL), was selected as the manufacturing process for the development of the advanced alumina core formulations. Gel casting was selected because it is a low-pressure process and has similar fabrication steps to existing processes used for the fabrication of silica cores. The similarity of the process steps for silica and alumina, plus the use of low pressure, means that little or no capital investment will be required for the introduction of the alumina core into manufacturing. The process map for the fabrication of the alumina core accompanied by two different core geometries produced by the gel casting process is shown in Figure 1. On the right side of the process map is shown the prototype serpentine core used for verification of cores suitability for use with superalloys of GTD-111 and single crystal N5.
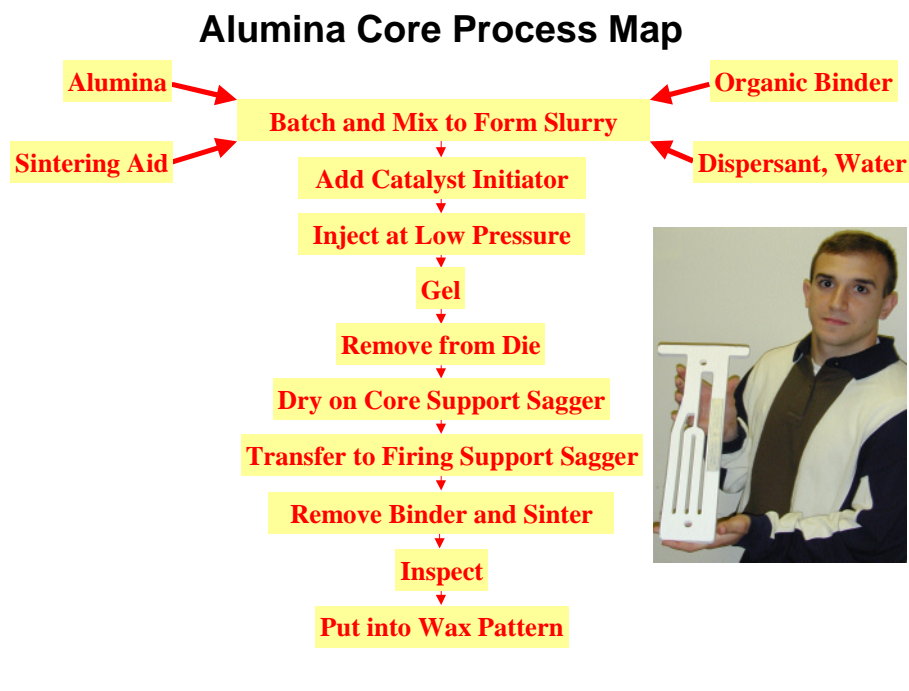
Alumina Core Process Map

Figure 1. Alumina core process map.

1.2 Alumina Core Development Technical Progress

Development of the Gel Casting Process. Short cycle time is important in the core manufacturing process, but is bounded by the need for some minimum working time prior to crosslinking of the monomer. The maximum allowed cycle time for core injection, monomer gelation, ejection, and die cleaning was set at 55 minutes as an upper specification. A lower specification set by the working time of the ceramic mix was set at 10 minutes. Early experiments found that occasional pre-mature gelation occurred before core injection. A list of potential causes that effect gelation was created, and six factors were selected for a ½-factorial experiment. The six-factor ½-factorial DoE was completed to determine the factors that statistically effect the time required for gelation or crosslinking of the monomer. The factors selected included: the amount of crosslinking inhibitor, the amount of sintering aid, the amount

of catalyst, the temperature of the room during mixing, the gelation temperature or die temperature, and the thickness of the samples. The samples for this study consisted of 3-inch diameter disks that were varied in thickness from ½ inch to 1 inch. The amount of time for gelation was determined experimentally by monitoring the temperature of the ceramic slurry after injection with a type K thermocouple. The maximum in the exotherm during gelation was taken as the gel time. The results are shown in Figure 2. Control of the two most significant factors, gelation and room temperature, has made possible the needed manufacturing control. Sample thickness was not a statistically significant factor and is therefore not shown in Figure 2.
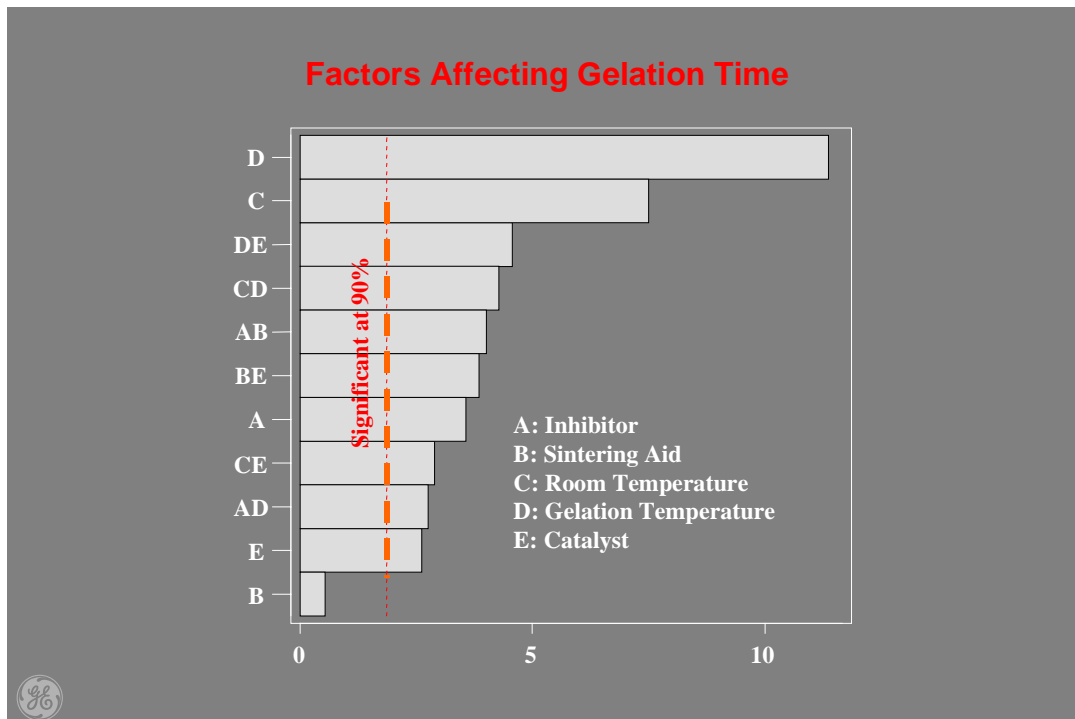

Figure 2. Gel time factors.

Shrinkage reproducibility. Development of the gel casting process was the primary focus of prior batches; these batches were not focused on core reproducibility. However, these batches served as a valuable database to determine the factors to be included into a DoE aimed at improving the shrinkage reproducibility to the required levels. A cause and effect diagram for shrinkage reproducibility was developed and is shown in Figure 3. Statistical analysis of the historical data was done using ANOVA, Regression analysis, and a custom DoE response surface. Based on the statistical analysis and the cause and effect diagram a 5-factor ½-factorial design with four center points was selected as a tool for improvement of the shrinkage reproducibility. The factors selected for study included: furnace heating rate, volume % solids in the injection slurry, the time at temperature for gelation or oven temperature, two different compositions, and mixing time of all components prior to injection. At each point of the DoE, 20 samples - with dimensions 50mm long by 12 mm wide by 6mm thick - were fabricated and sintered. The sintering shrinkage of each bar was measured and a standard deviation calculated. The standard deviation of the batch was taken as a measure of the shrinkage reproducibility. The results are

summarized in the Pareto chart shown in Figure 4. The volume percent solids and the mixing time were the main effects affecting the shrinkage reproducibility. The results confirmed that short mixing times lead to inhomogeneity and variable shrinkage; therefore, long mixing times were preferred. In addition, high solids loadings were preferred because the total shrinkage and shrinkage variability was reduced. The interaction terms such as mixing time * heating rate while statistically significant are not technically understood at this time.
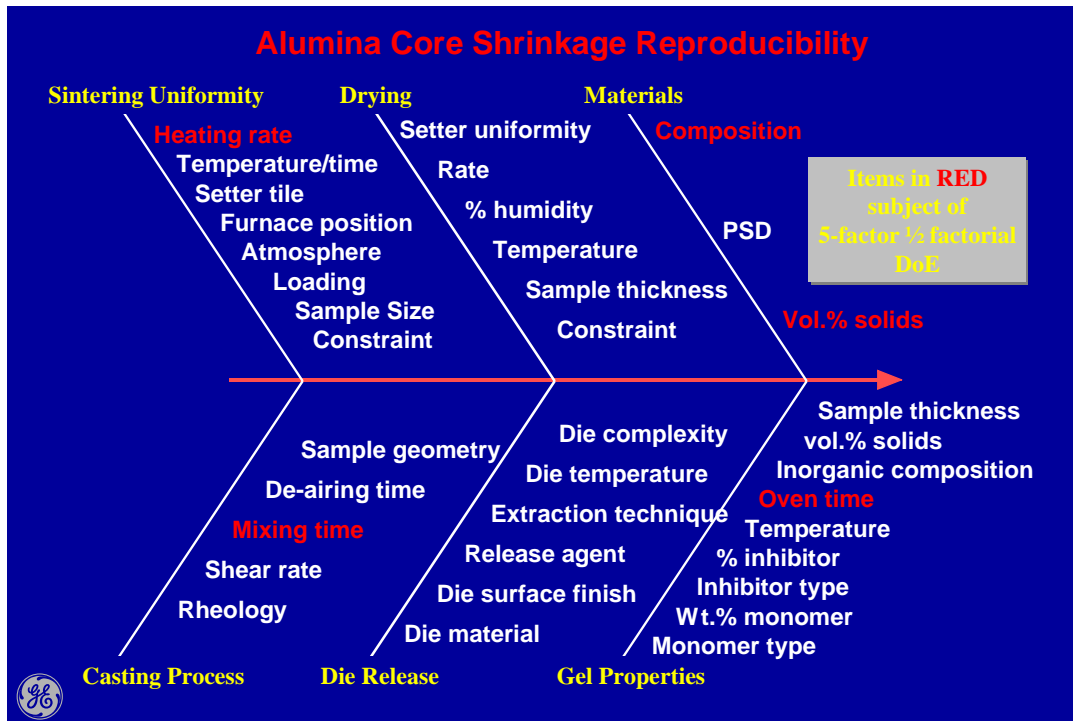

Figure 3. Cause and effect diagram for shrinkage reproducibility.

Alumina core composition development. The development of an alumina core based on Russian formulations required identification of US raw materials with similar properties to Russian raw materials. The selection criteria for the alumina to be used were based on the firing shrinkage, the visual appearance of the samples, and fired density of the samples. A mixture Design of Experiment (DoE) was defined to determine the optimum levels for each of the components. The mixture DoE is a 4-component D-optimal mixture for fitting a Scheffe model and includes all two-way nonlinear blending effects. The DoE consisted of a minimum of 10 runs. Five additional runs are included to check for lack of fit and 3 repeat runs were included to estimate the pure error of the experiment. The four components in the DoE consist of AA 1, 2, and 3 plus a component consisting of fused alumina. The fused alumina consists of 4 different mesh sizes of fused alumina, which are kept in a constant ratio to allow the DoE to treat the fused alumina mixture as one component.

Tooling that produces test bars of sizes 50mm by 12mm by 5mm, 40mm by 12mm by 5mm, and 150mm by 15mm by 6.4mm was fabricated. From each composition twenty 50mm bars, twenty 40mm bars and five 150mm bars are injected. The following attributes were measured for each composition: porosity after 1675°C, elastic modulus and creep rate.
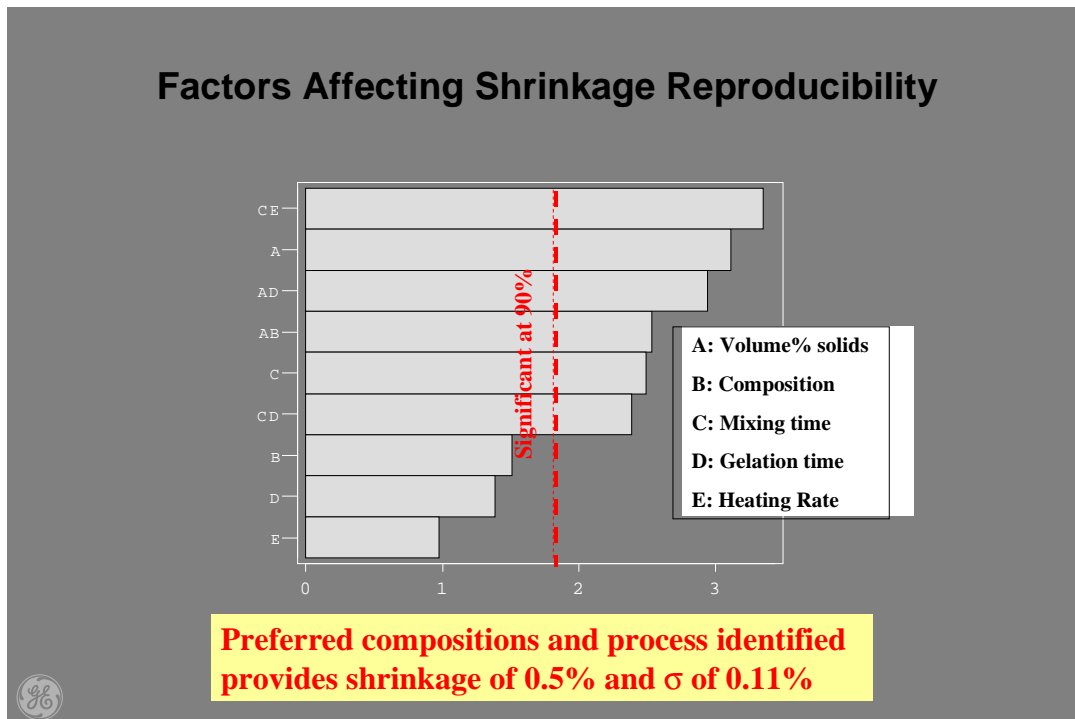
Factors Affecting Shrinkage Reproducibility

A: Volume% solids
B: Composition
C: Mixing time
D: Gelation time
E: Heating Rate

Significant at 90%

Preferred compositions and process identified provides shrinkage of 0.5% and σ of 0.11%

Figure 4. Factors affecting shrinkage reproducibility.

Creep rate, elastic modulus, and compressive strength as a function of core composition. An important attribute for core performance is the ability of the core to accommodate and relieve the strain energy that develops during cooling of the core as a result of the thermal expansion mismatch between the ceramic core and the metal casting. If the stain is not relieved, the stress can build to a large enough value to crack the casting or to cause extra grains to nucleate in a single crystal casting. Three potential methods of strain relief have been identified these include crushing of the core by the metal during cooling, elastic deformation of the core, and creep deformation of the core. Of course creep deformation is not desirable. For the best dimensional stability, a high resistance to creep is desired. Therefore, the best core compositions will have a low elastic modulus, a low compressive strength, and a high creep resistance. Work concentrated on the measurement of creep rate, elastic modulus, and compressive strength of the core as a function of composition. Promising core compositions have been selected. An optimum sintering temperature was selected based on the creep rate of the core.

Experimental procedure for elastic modulus measurement. One to three specimens of each core composition were tested by first measuring the mass, dimensions and resonant flexural frequency for the dynamic Young's modulus determination. The resonant flexural frequencies were measured by suspending the rectangular beam specimens from support wires at the node positions for the fundamental flexural resonance. The specimens were excited by impacting the center of the beam with a small zirconia sphere in a manner similar to that described in the upcoming ASTM standard C-1259-94, "Elastic Modulus by Impulse Excitation of Vibration". The resulting resonant vibrations were sensed with an acoustic microphone, also similar to that described in the ASTM standard. The resonant

frequencies of the specimens were determined by feeding the microphone output to a digital storage oscilloscope with fast Fourier transformation capabilities. The resonant frequency for the fundamental mode of flexural vibration, along with specimen mass and dimensions, were then used to calculate the in-plane Young's modulus of the core material in a stress-free state.

Experimental procedure for measurement of core crushability. Each sample was sintered at 1675°C prior to testing. In addition, the dimensions of rectangular bars from each core composition were recorded before and after testing. The sample bars were sealed in rubber bags, the air was evacuated from the rubber bag, and the sealed bag with sample was placed into an isostatic press. The press was pressurized to in stages to 10,000, 20,000 and 25,000 psi. After each stage, the samples were removed from the press dimensions measured and then replaced into the press. After each stage some of the samples were crushed to powder. Only samples that did not crush were replaced in to the press for testing at higher pressure.

Experimental procedure for creep. The creep rate of the alumina core was measured in four-point bend. The lower span was 44.5 mm and the upper span was 12.5 mm. The nominal sample size was 50 mm by 12 mm wide by 5 mm thickness. Prior to testing each bar was sintered to 1675°C with a 2-hour isothermal hold at 1675°C. Sample dimensions were measured for each bar and the load needed to provide a 30 psi stress was calculated. Each bar was loaded and weighted to provide a stress of 30 psi. While loaded each sample was heated in vacuum at 200°C/hr to 1565°C for a 2-hour hold at temperature. The hot zone temperature measurement was made with W-Re thermocouples after calibration with type S Pt-Rh thermocouples. Temperature measurements for both sintering and creep testing are accurate to within ±2°C. After testing the deformation was measured ±001 inches and the creep rate was calculated using a modification of the equations developed by Hollenberg *et. al.* [G. W. Hollenberg, G.R. Terwilliger and R.S. Gordon. 1971. Calculation of stresses and strains in four point bending creep tests. *J. Amer. Ceram. Soc,* 54, 196-199]. The equations used for calculation of strain as a function of sag deformation are shown below. To obtain a creep rate the strain was divided by the time of the test at the top temperature. In addition for this study the creep exponent for assumed to be 1. A creep exponent of 1 assumes that the dominant creep mechanism is viscous flow.

$$E_{max} = \left[\frac{(4h(N+2))}{a^2(N+2)+2(L-a)[L+a(N+1)]} \right] yc$$

For n = 1

$$E_{max} = \left[\frac{12h}{(3a^2+2(L-a)[L+2a])} \right] yc$$

where:

$\qquad E_{max} =$ max strain in outer fiber

h   =   bow thickness
a^2 =   inner span length
y   =   deflection at load points
yc =   deflection to beam center
ye =   deflection between upper load points and bar center
n   =   the creep exponent

An initial screening test using alumina core samples supplied to GE in 1997 by VIAM were used to develop the sintering and test conditions. The VIAM cores were sintered at 1600, 1675 and 1775°C prior to sag testing. After sintering the porosity of each sample was determined using the standard Archimedes immersion density technique. Spriggs and Vasilos [R. M. Spriggs and T. Vasilos. 1964. Functional relationship between creep rate and porosity for polycrystalline ceramics. *J. Amer. Ceram. Soc.,* **47**, 47-48] found that the creep rate of polycrystalline alumina is proportional to $1/(1-P^{0.667})$ where P is the porosity. P can have values from 0 to 1 with 1 representing 100% porosity. The results on the VIAM cores were plotted in Figure 5 as a function of the porosity parameter $1/(1-P^{0.667})$. An excellent least squares fit was found for the data with a $R^2=0.93$. As expected the lowest creep rate occurred at the highest sintering temperature. However, 1675°C was selected as the sintering temperature for all subsequent tests because it is the highest practical temperature that can be achieved with existing equipment at the major US core vendors.
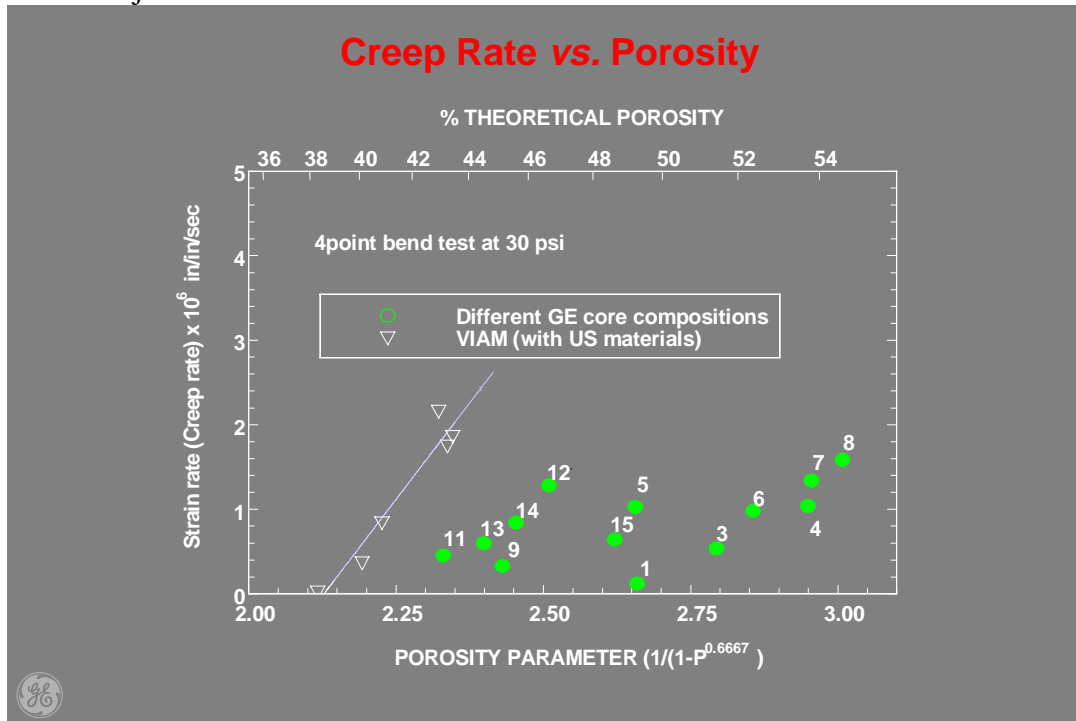

Figure 5. Creep rate *vs.* porosity.

Experimental results for elastic modulus, creep rate, and crushability. The results of the elastic modulus, creep rate and crushability tests are shown in Table II as a function of the composition. The creep rate as a function of porosity and composition is shown in Figure 5. The results show that the best GE formulations have equal or lower creep rates than samples produced at VIAM with a higher

desirable porosity. A transfer function was obtained for elastic modulus, creep rate and porosity. The predicted values based obtained from the transfer function are compared to the measured values in Figure 6.
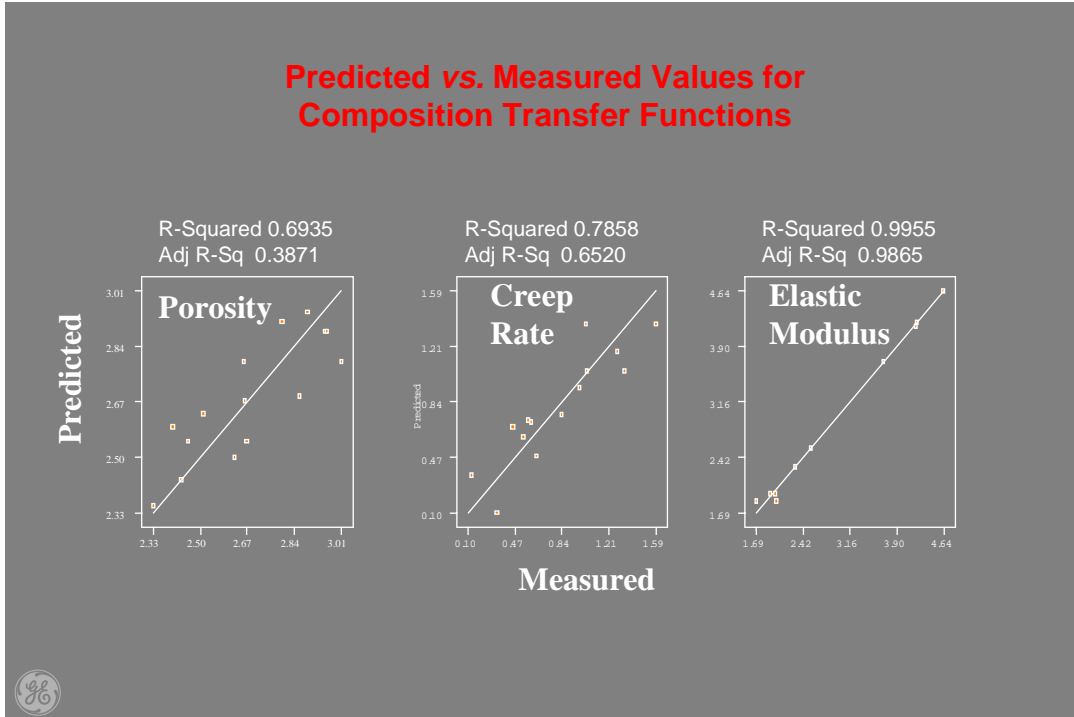

Figure 6. Comparison of predicted *vs.* measured core properties.

The crushing pressure in the table is the pressure at which the sample was converted to a pile of powder. Design for Six Sigma Analysis is in progress to determine acceptable lower/upper limits for each of these values. Analysis of the existing data with the following the criteria of low creep rate, and high porosity have led to establishing a preferred proprietary composition.

Core process scale-up. A prototype core design has been selected for further development of the core manufacturing process. This core design will be used to validate the process before more complex geometries are fabricated. The die design is shown in Figure 7. The design requirements for the prototype core included:
1. Design features with enough complexity to model production parts;
2. A simple flat shape on which distortion and shrinkage is easy to measure;
3. Compatibility with existing equipment for core manufacturer at GE.

Several features of the die are particularly well suited for advanced core development. The complex serpentine features of the core are designed to validate the development of the low-pressure injection process. In addition, the serpentine features of the core provide the needed difficulty in geometry for leaching trials. The core is flat without curvature in the thickness direction. The flat design makes unambiguous the determination of distortion during subsequent process. In fact, the flat design will

make it difficult for distortion to be hidden in the complex curvature that is present in production tooling. The distortion measurements will have increased sensitivity because of the flat design and as a result distortion and shrinkage are easily tracked at each stage of the process. This sensitivity has aided in the reduction in drying shrinkage of the core to less than 0.03% in/in. In addition, two holes in the core have been added at the top and the bottom of the core. These holes which are not part of production cores will increase the sensitivity of the shrinkage measurements at each stage of the process. A representative core fabricated from the die is also shown in Figure 7.
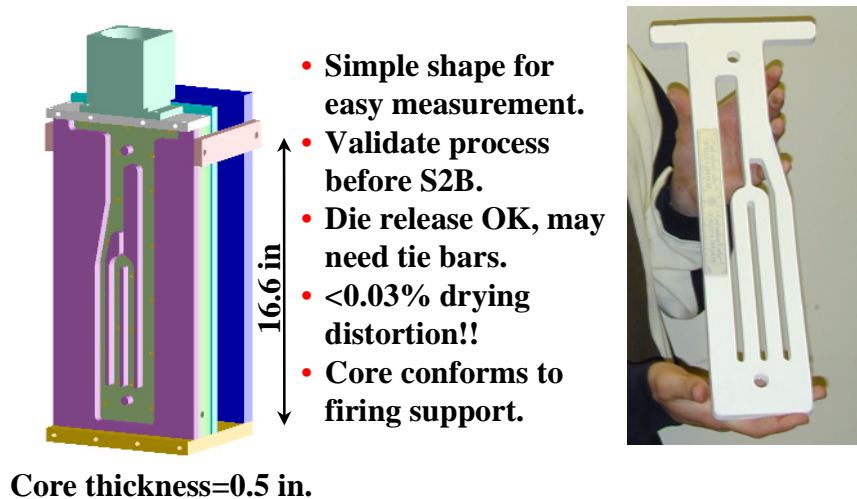
Core Process Scale Up

- Simple shape for easy measurement.
- Validate process before S2B.
- Die release OK, may need tie bars.
- <0.03% drying distortion!!
- Core conforms to firing support.

16.6 in

Core thickness=0.5 in.

Figure 7. Prototype core design.

Casting results. The first casting trails using the core formulations developed in this study are shown in Table III. The casting results show that the sintering temperature of the core was an important variable. Low sintering temperature lead to low mechanical strength and premature failure of the core during processing. The designation "core 470" is for the flat prototype core. Cores that were sintered at 1620°C and above survived the casting in directionally solidified GTD-111. The resulting castings were acceptable.

Leaching results. The alumina cores that survived the casting trials were leached using an autoclave caustic solution at GE and in a proprietary leaching procedure at PCC airfoils. The GE results will be described first. Two leaching trials were made both resulting in partial core removal. The depth of the core removal from the casting was measured and the time for total core removal estimated by assuming that the core removal rate was either step wise linear or diffusion controlled. Use of a step-wise linear transfer function yields a core removal rate of 12 mm/h, while the diffusion controlled transfer function yields a removal rate of 8 to 22 mm/h $^{0.5}$. These removal rates correspond to leaching times between 24 and 150 hours for a second stage gas turbine blade. A similar leaching trial was done at PCC airfoils using a PCC proprietary leaching system. The leaching rate was step-wise linear and the core was

totally removed from the casting. An estimate of the leaching time of 50 h was made for complete leaching of a second stage blade.

Table II

Composition or run number	Creep Rate (in/in/s)	Elastic Modulus (Mpsi)	Crushing pressure (psi)
1	0.12	5.547	20,000
2		3.301	10,000
3	0.54	4.617	20,000
4	1.04	2.642	10,000
5	1.03	2.749	10,000
6	0.98	5.688	10,000
7	1.34	2.630	10,000
8	1.58	2.795	10,000
9	0.29	4.896	10,000
10		5.148	20,000
11	0.45		25,000
12	1.28	3.711	10,000
13	0.60		25,000
14	0.84		10,000
15	0.64		20,000

Table III.

Casting Results

Part ID	Sintering Temperature	Metal Wall Thickness (inches)	Wax Removal	Casting Results
Five bars six″ long	1675°C	0.2 to 0.25″	OK	OK
18″ long, ¾″ dia. rod	1500°C	0.150″	OK	Broke
18″ long, ¾″ dia. rod	1620°C	0.150″	OK	OK
470 core	1500°C	0.20″	Broke	Not cast
470 core	1500°C	0.150″	OK	Broke

Low sinter temperature resulted in core breakage

Alumina core cost analysis. The cost analysis for the production of a second stage alumina core was estimated. Assumptions were made for the cost of labor with benefits, the cost of electric power for the core sintering, cycle time/core, and a core yield of 75%. The cost of capital equipment and depreciation was not included. The yielded alumina core cost was $94.32. This initial cost estimate indicates that the alumina core is not excluded based on the economics of manufacture.

2. Focus of Casting Research

A proficient nucleation of grains at the bottom of a mold is necessary to grow oriented [100] grains during directional solidification (DS). Preliminary results indicated that grain nucleation as well as thermal gradient could be issues in the LMC process for large DS industrial gas turbine buckets. Two sets of experiments were carried out before trial casting of prototype 9G-machine stage-2 buckets (9G-S2B). In the first set of experiments, a laboratory-scaled conventional DS furnace was used to study the effects of seed material, geometry, and temperature on grain nucleation and [100] texture development. In the second set of experiments, the LMC pilot furnace was used to study the effect of mold start position and melt pour temperature on grain nucleation and dendrite arm spacing. Knowledge obtained from these experiments is used for casting of 9G-S2B.

2.1 Laboratory DS Furnace Seeding Experiments

In these experiments, the mold was a dense alumina tube with one end sealed off with a disk of seed material. This mold assembly is positioned on a water-cooled copper pedestal, seed down. After preheating and filling with molten GTD111 alloy at about 1550°C, the mold was withdrawn from the heater at the rate of 5mm/min (12 in/h), producing DS samples about 1 inch in diameter and 5 inches long.

A variety of seeds, including two seed materials, two surface preparations, and two levels of thickness, have been evaluated in the format of design of experiments, Table IV. Characterization of the casting samples include surface grain etch, metallography, and EBSP analysis. The EBSP technique allows a qualitative assessment of how the DS grains are aligned with the [100] orientation. The latter result is included in Table IV.

Table IV

Exp. No.	Seed Type	Surface Preparation	Seed Thickness	[100]Texture (score 1-10)
1	material1	flat	0.25"	10
2	material1	flat	1"	9
3	material1	grooved	1"	9
4	material1	grooved	0.25"	10
5	material2	grooved	0.25"	7
6	material2	grooved	1"	10
7	material2	flat	1"	8
8	material2	flat	0.25"	8

Table IV shows that seed material is the primary factor controlling the [100] texture development. Seed material 1 (experiments 1-4) tends to produce better texture than seed material 2 (experiments 5-8). Seed thickness appears to be a secondary factor. When the preferred seed material 1 is used, a thinner seed (experiments 1, 4) produces slightly better texture than a thicker seed (experiments 2, 3). The observed seed thickness effect suggests that a colder seed (as in the case of the thinner seed close to the chill) is preferred over a hotter seed (as in the case of the longer seed well into the mold heater). Surface preparation of the seed

2.2 LMC Mold-470 Casting Experiments

In these experiments, an alumina-shell mold (mold-470) without special seeding arrangement was used for casting in the LMC pilot furnace. The mold was first positioned in a mold basket, preheated in a heater, and filled with molten GDT111 before being lowered into a vat of molten aluminum at the rate of 5mm/min. The resultant casting was about 470mm long, having the shape of a step block with thickness ranging from 15mm to 85mm.

Two variables important to the nucleation and growth of the DS structure are evaluated in the format of design of experiments, Table V. First, the mold was either preheated at a "hot start" position well inside the mold heater, or a "cold start" position with the bottom of the mold immersed in the aluminum bath, Figure 8. The "hot start" keeps the bottom of the mold above the melting temperature (typically ~1450°C) before the melt is poured, while the "cold start" maintains the mold bottom below the melting temperature (typically 1000-1300°C). Second, the melt was either poured "hot" at ~1550°C, or "cold" at ~1450°C. The effects of the process variations were characterized by etching the as-cast surfaces for nucleation, Figure 8 and by metallography on transverse sections for dendrite arm spacing Figures 9. The characterization results are included in Table V.

Table V

Casting No.	Mold Start Position	Melt Pour Condition	Nucleation (score 1-5)	DAS (microns)
LMC-6	hot	hot	1	340
LMC-13	cold	hot	3	425
LMC-9	cold	cold	5	571
LMC-3	hot	cold	2	637

Table V shows that mold start position is the primary factor controlling grain nucleation. "Cold start" (LMC-13 and -9) tends to result in more nucleation and better DS structure than "hot start" (LMC-6 and -3). Melt pour temperature is a secondary factor regarding grain nucleation, with "cold pour" (LMC-9 and –3) being preferred over "hot pour" (LMC-6 and –13). Also, Table V shows that dendrite arm spacing is primarily controlled by the pour condition, but not the mold start position. The "hot pour" condition (LMC-6 and –13) generally results in smaller DAS compared with the "cold pour" condition (LMC-9 and –3).
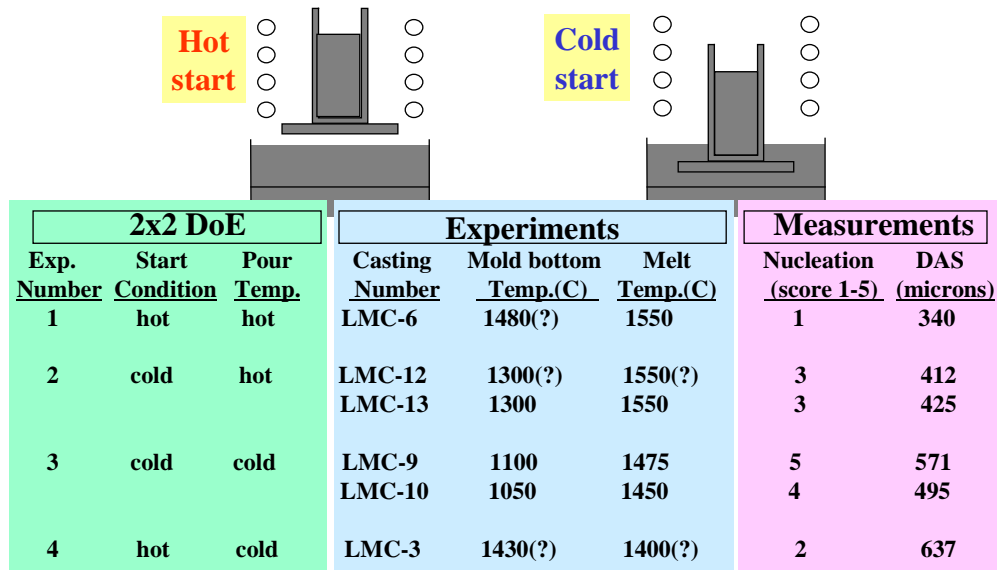
LMC Mold-470 Nucleation DoE

Hot start   Cold start

2x2 DoE			Experiments			Measurements	
Exp. Number	Start Condition	Pour Temp.	Casting Number	Mold bottom Temp.(C)	Melt Temp.(C)	Nucleation (score 1-5)	DAS (microns)
1	hot	hot	LMC-6	1480(?)	1550	1	340
2	cold	hot	LMC-12	1300(?)	1550(?)	3	412
			LMC-13	1300	1550	3	425
3	cold	cold	LMC-9	1100	1475	5	571
			LMC-10	1050	1450	4	495
4	hot	cold	LMC-3	1430(?)	1400(?)	2	637

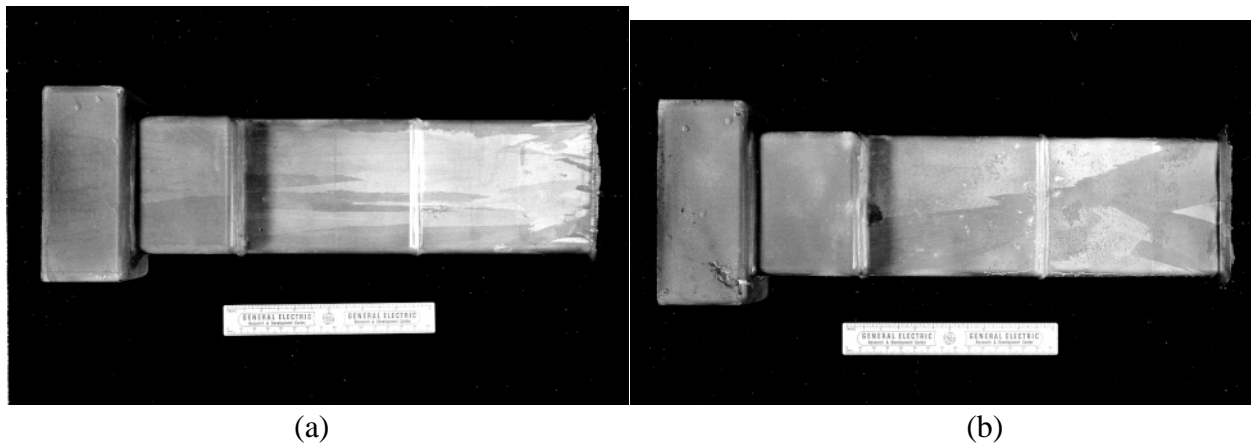Figure 8. Hot and cold start experiments.

(a)   (b)

Figure 9. Mold 470 macrostructure: (a) cold start; (b) hot start.

It is noteworthy that among the mold-470 castings studied above, LMC-3 is the only one showing freckle defects after the surface etching. The freckle chains appear on the largest step block section of the casting (section 3). A detailed study of the DAS was carried out to understand the defect formation. Table VI shows the DAS measured at the different sections of the castings. Using the correlation between DAS and cooling rate, and knowing the withdrawal rate (R) is at 5 mm/min, the thermal gradient (G) experienced at each section can be estimated and plotted in a gradient-versus-withdrawal rate process map, Figure 10. As seen, the data points suggest a freckle criterion near GxR=0.01°C/sec.
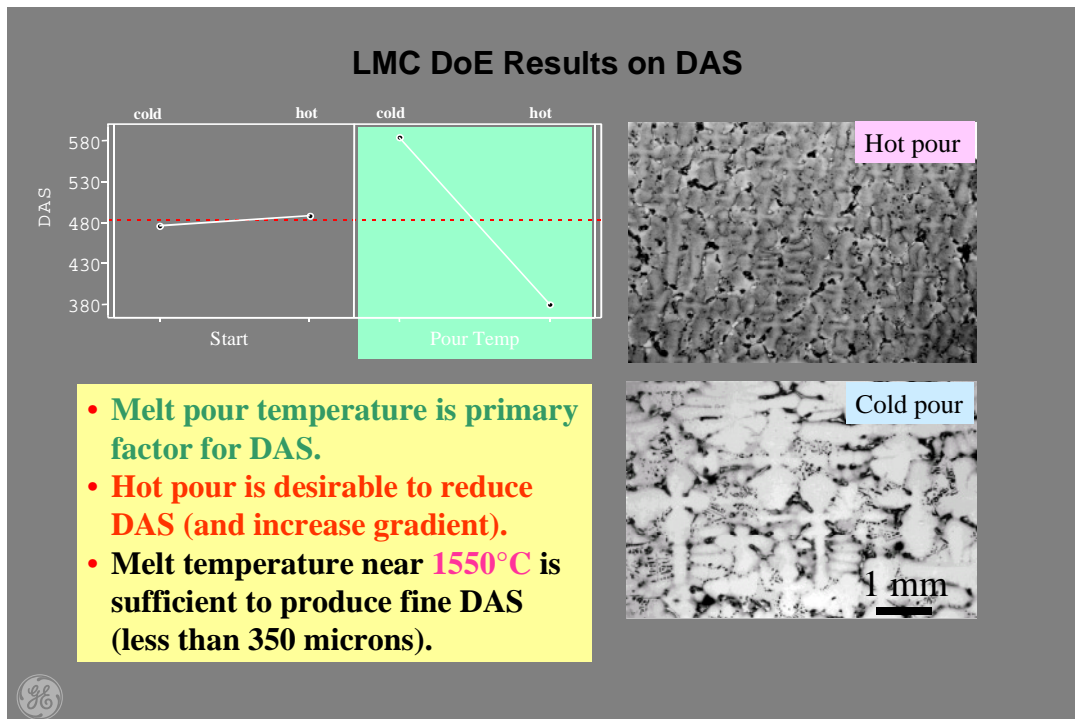
Figure 9. Dendrite arm spacing as function of start conditions.

Table VI

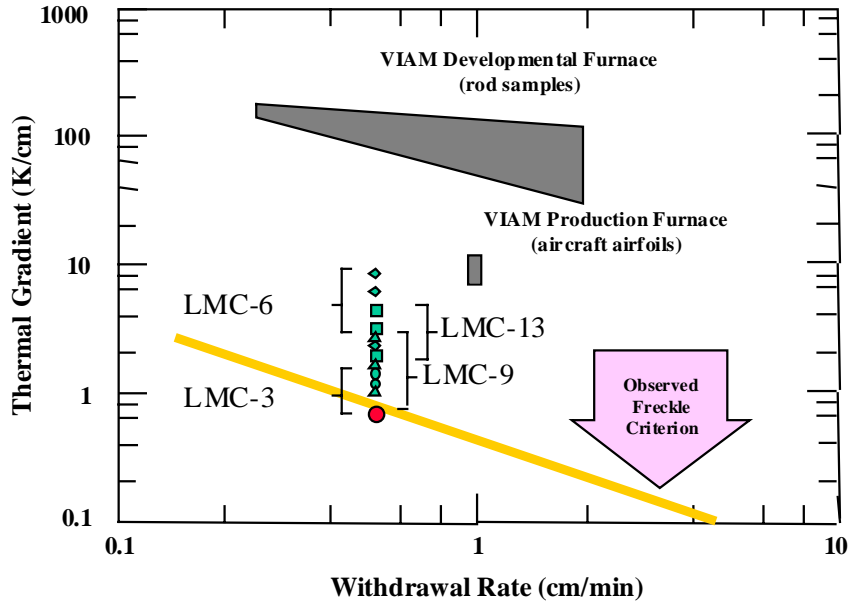| Casting No.	Section No.	DAS (microns)	Estd G (C/cm)	Freckle Formation
LMC-6	1	305	9.4	no
	2	340	6.7	no
	3	474	2.5	no
LMC-13	1	400	4.2	no
	2	425	3.5	no
	3	523	1.8	no
LMC-9	1	452	2.8	no
	2	571	1.4	no
	3	664	0.9	no
LMC-3	1	581	1.3	no
	2	637	1.1	no
	3	712	0.7	yes

Figure 10. DS process map showing LMC castings are outside region prone to freckle defects.

2.3 LMC 9G-S2B Trial Castings

The mold for this prototype component was about 750mm long with the airfoil-tip down. The experimental setup and procedure are similar to the mold-470 experiments described above.

The results from the two sets of experiments above define certain mold preheat and melt pour conditions for casting 9G-S2B in the LMC furnace. As seen in Table VII, the preferred conditions of "cold start" and "hot pour" are used in the first two trials (LMC-16 and 17). Each of those casting trials resulted in a run-out, and only a section of the airfoil was cast. In the third trial (LMC-19), the mold pre-heat and melt pour temperatures were lowered, and the run completed without a run-out.

Table VII

Casting No.	Mold Preheat Temperature (C)	Mold Start Condition	Melt Pour Temperatur (C)	Casting Completed
LMC-16	1550	cold	1550	~5" of airfoil
LMC-17	1550	cold	1550	~10" of airfoil
LMC-19	1500	cold	1450	whole

Figure 10. LMC-19

Figure 10, right, shows the LMC-19 casting with surface grain etched to show the successful development of DS structure. A careful examination of the etched surface showed no freckle chain formation even in the areas with the largest cross sections.

Metallography from the airfoil section of the LMC casting shows that the dendrite arm spacing is about 303 microns, which corresponds to a gradient of 9.4°C/cm. This gradient value is well above the freckle criterion determined in Figure 9.

3. Summary

An alumina core and binder process window has been identified with core mechanical properties designed to meet the casting needs. The core meets industry benchmarks for shrinkage and shrinkage reproducibility. A prototype core die has been designed and built; and the first prototype cores fabricated and sintered. Optimization of the casting temperature was shown to be important in achieving successful castings. Castings were successfully leached in times that we be acceptable for manufacturing cycle time. A cost estimate of producing an alumina core was made.

Several LMC processing variables have been examined in order to control the nucleation and growth of DS grain in large gas turbine components. From the designed experiments carried out, the variables of mold preheating position and melt pour temperature was identified to be the critical parameters controlling the DS structure. The "cold start" and "hot pour" conditions are the preferred conditions to produce sufficient number of [100] grains aligned in the growth orientation. Casting of large stage-2 bucket for prototype 9G machine has been demonstrated.